Electronic supplementary information (ESI)

This document is devoted to the theoretical part of the work which implies a large and exhaustive exploration of the potential energy surface.

I.1. Theoretical methodology

The procedure used in the present work has been described in detail in a previous article [1]. The exploration of the potential energy surface of the complexes is divided into two different steps already described elsewhere [2]. We have first determined all the minima of the potential energy surface by means of a semi-empirical method developed by Claverie [3] and extended by Brenner et al. [4], in which only the intermolecular coordinates are optimised. Secondly we have performed DFT calculations for a full optimisation of the most stable isomers resulting from the semi-empirical method as well as the calculation of the associated harmonic frequencies. For a better evaluation of the relative energy of the complexes, the most pertinent geometries have been optimized at the MP2 level of theory to take into account the dispersive interactions.

The semi-empirical method is based on the perturbation exchange theory [4,5]. It rests on a description of the interaction energy as a sum of four terms (electrostatic, repulsion, polarisation and dispersion) which can be written analytically as a function of the intermolecular distances, combined with a whole exploration of the potential energy surface. The potential energy surface is first explored by simulated annealing with the Metropolis algorithm [6]. Secondly, an energy optimisation of all the minima found in the simulated annealing step is performed. At the end of this optimisation, we get the different components of the interaction energy for each minimum of the potential energy surface.

The twenty most stable complexes resulting from the previous step are fully optimised using DFT calculations. The calculations have been performed using (1R,2S)-(+)-cis-1-amino-2-indanol and the two enantiomers of methyl-lactate. To ensure a full exploration of

the potential energy surface, the following procedure has been followed: when a structure has been found with one of the enantiomers of ML and not the other, the equivalent structure has been created by interchanging the hydrogen and methyl substituents of the asymmetric carbon, and further optimised. When appropriate, starting structures were also manually modified to create an analogous structure containing an other conformer of the constituents. As mentioned above, the semi-empirical method used in the first step of the calculations does not allow for modification of internal degrees of freedom. Chemically relevant structures involving large molecular modifications have therefore been created manually, guided by chemical intuition, and optimised. All the calculations have been carried out with the Gaussian 03 software package [7]. The complexes are locally optimised employing the B3LYP density functional with the standard 6-31G(d,p) basis set of Gaussian. The BSSE is also calculated, following the counterpoise method of Boys and Bernardi [8]. It turns out that the BSSE deduced from the counterpoise method is overestimated. As suggested in previous work [9], half the BSSE value is used as a correction. Finally, the harmonic frequencies have been obtained at the same level of theory.

Last, the most promising complexes are re-optimised at the MP2/6-31G(d,p) level of theory. The BSSE and the deformation energy are also calculated at this level of theory. The deformation energy given in what follows is the energy difference between the energy of the molecule in its optimised geometry and the energy of the molecule in the geometry it adopts in the complex. A given complex involves deformation energy for each of its sub-unit. We will consider that the highest value from those obtained for each of the sub-units is the important parameter and we will give this value only in what follows. The binding energies (BE) given in the text and in the tables are those obtained at the MP2/6-31(d,p) level of theory, including half the BSSE. The most stable form of the complex may involve sub-units, which are not the most stable forms of the individual components but conformations

corresponding to secondary minima of the potential energy surface. The given binding energies correspond to the dissociation to the closest stable conformers.

The size of the systems precludes any frequency calculation at the MP2/6-31(d,p) level of theory: all the simulated vibrational spectra are obtained at the B3LYP/6-31G(d,p) level and corrected by a scaling factor of 0.96 in the νCH) and ϒOH) region (values given in the text and in the tables).

I.2. Results

The complexes have been calculated starting from the two stable conformers AI_I and AI_{II} of (1R,2S)-(+)-cis-1-amino-2-indanol and the three conformers (Syn, G, G') of methyl lactate described above in their R and S enantiomeric forms. In what follows, we will describe the most stable calculated complexes, according to their hydrogen-bond pattern. These complexes will be divided into four different families, called hereafter head-to-head, insertion, addition and cycle. These families are schematically depicted in scheme 2 in the article. In what follows, we call heterochiral or RS the complexes built from (1R,2S)-(+)-cis-1-amino-2-indanol and (S)methyl lactate. We will describe in detail the structure of the calculated complexes belonging to each of these families for the RS diastereoisomer. Then we will describe more rapidly the results obtained for the RR diastereoisomer, and emphasize the differences relative to the RS complex.

The complexes with binding energies larger than 10 kcal/mol are listed in table S1, together with their deformation energies and harmonic frequencies of significant intensity. Complexes with binding energies lower than this limit are also included in table S1 if their diastereoisomer has a binding energy higher than 10 kcal/mol.

I.2.a. RS complexes

- Head-to-head structure

The "head to head" structure, schematically depicted in scheme 2a-, results from the opening of the two intramolecular hydrogen bonds to allow the formation of two strong intermolecular hydrogen bonds. This structure can be formed with the Syn form of methyl-lactate as well as G or G'. The OH group of methyl lactate (called OH_{ML} hereafter) points towards the nitrogen atom of AI and the OH group of AI (called OH_{AI}) points toward the oxygen of the carbonyl group (called $O{=}C_{ML}$) or the ester group (called OCH_{3ML}) of methyl lactate, depending on whether AI is complexed to the Syn or G (G') conformer of methyl lactate. Because of the formation of strong intermolecular hydrogen bonds, the head-to-head structures have the highest binding energy of all the calculated complexes. On the other hand, the opening of two intramolecular hydrogen bonds results in large deformation energy. The calculated spectra for this family display an intense red-shifted transition, characteristic of a strong OH_{ML}…N interaction, and a band typical of an OH_{AI} … O_{ML} interaction.

The head-to-head family is divided into two sub-families. In the first one, the two intermolecular hydrogen bonds are really linear. In the second one, the OH_{AI}….O_{ML} is not linear because the OH_{AI} donor is shared between the two oxygen atoms of methyl lactate (fig. S1a), resulting in a so-called bifurcated hydrogen bond. This kind of subdivision is also true for the "cycle" family described later.

The most stable among all the calculated complexes (head to head bifurcated/AI_{II}-G') belongs to the bifurcated type and is built from AI_{II} and the G' conformer of methyl lactate (fig. S1a). Its binding energy is 12.59 kcal/mol and the deformation energy of methyl lactate amounts to 1.99 kcal/mol. Its calculated vibrational spectrum (see fig. S2a-) displays two main transitions located at 3153 and 3537 cm^{-1} and associated with the OH groups of methyl-lactate and AI, respectively.

The second most stable complex (head to head/AI_{II}-Syn) exhibits a "head to head" structure between AI_{II} and the Syn conformer of methyl lactate (fig. S1b-). Its binding and deformation

energies amount to 11.93 and 2.83 kcal/mol, respectively. The associated vibrational frequencies at 3139 and 3521 cm^{-1} are located on the OH groups of methyl lactate and AI, respectively (fig. S2b). As the $OH_{AI}…O_{ML}$ is not bifurcated, in contrast with the previously described complex, the associated vibrations are slightly shifted down in energy (3521 compared with 3537 cm^{-1}).

The next most stable head to head structure is obtained with AI_I (head to head/AI_I-Syn fig. S1h) Its binding and deformation energies are 10.80 and 3.19 kcal/mol, respectively. The calculated frequencies associated with this geometry are given in table S1, they are located at 3139 and 3534 cm^{-1}. These frequencies are similar to those calculated for the equivalent complex containing AI_{II}. It is to be noticed that this complex is not the most stable one obtained for the AI_I conformer. As we will see later, the insertion bifurcated/AI_I-G is more stable than the head to head/AI_I-Syn.

The last "head to head" structure with a binding energy above 10 kcal/mol contains AI_{II} and the G conformer of methyl lactate (fig. S1k-). Its binding and deformation energies are 10.23 and 1.81 kcal/mol respectively. The calculated vibrational frequencies associated with this structure are 3229 and 3563 cm^{-1} (fig. S2k-). They are higher in energy than in the equivalent complex containing the Syn conformer of methyl-lactate. This is especially true for the lower-energy one, corresponding to the OH_{AI} stretch, because the OH_{AI} ….OCH_{3ML} interaction is looser than the OH_{AI} ….$O{=}C_{ML}$ hydrogen bond.

- Insertion structure

The "insertion" structure (scheme 2b-) corresponds to the insertion of the OH group of methyl lactate into the intra molecular hydrogen bond of AI. It involves the formation of two strong $OH_{ML}…N$ and $OH_{AI}…OH_{ML}$ intermolecular hydrogen bonds, with concomitant opening of the intramolecular hydrogen bonds. The binding energy is large, only slightly

lower than that of head to head structures. This insertion structure is reminiscent of one of those calculated, but not observed, for the AI hydrates [10].

The insertion/AI_{II}-Syn complex shown in fig. S1c- involves the Syn conformer of methyl lactate. The associated binding and deformation energies are 11.39 and 2.42 kcal/mol, respectively. The OH located on the methyl lactate is involved in the OH_{ML}…N hydrogen bond and its stretching mode frequency exhibits a very strong red shift down to the CH stretch region (3068 cm^{-1}). The other OH frequency (3506 cm^{-1}) is one more time typical of an OH_{AI}…OH_{ML} interaction (see fig. S2c-).

The insertion/AI_{II}-G complex shown in fig. S1d- has an "insertion" structure based on the AI_{II} and G conformers. Its binding and deformation energies are 11.38 and 1.81 kcal/mol, respectively. The associated frequencies (fig. S2d-) are localised at 3181 and 3522 cm^{-1}, as expected from the existence of two strong intermolecular OH_{ML}…N and OH_{AI}…OH_{ML} bonds. They are however slightly higher in energy than those calculated for the equivalent complex containing Syn methyl-lactate.

The next most stable complex is the first insertion complex obtained from the AI_I conformer of aminoindanol (insertion/AI_I-G). Despite being the most stable complex built from AI_I, it appears to be strongly less stable than those obtained with the AI_{II} conformer. Its geometry is depicted in fig. S1f- and its binding and deformation energies amount to 11.13 and 2.48 kcal/mol, respectively. The spectrum is depicted in fig. S2f-. The frequencies associated with this geometry are calculated at 3110 and 3525cm^{-1}. These frequencies are very different from those calculated for the equivalent structure containing AI_{II}, in particular the lower-energy one located on OH_{ML} is strongly shifted down in energy in the complex with AI_I.

A second insertion/AI_{II}-G complex (fig. S1g-) is obtained and will be called insertion/AI_{II}-G*bis*. Its binding and deformation energies are 10.87 and 1.57 kcal/mol, respectively. The frequencies associated with the two OH stretch modes are 3166 and 3488 cm^{-1} (see fig. S2g-).

An other insertion complex is obtained with AI_I (fig. S1j-). Its binding and deformation energies amount to 10.42 and 2.60 kcal/mol, respectively. This insertion/AI_I-Syn complex is formed between AI_I and the Syn conformer of methyl lactate. It differs from the other insertion complex containing AI_I by the fact that an additional intermolecular hydrogen bond takes place from one of the NH of the amino group to the oxygen atom of the carbonyl group of methyl lactate. Its calculated vibrational frequencies are located at 3044 and 3509 cm^{-1} (fig. S2j-). We can notice that the OH_{ML} stretch has the lowest frequency (3044 cm^{-1}) of all the calcutad. Indeed, OH_{ML} is strongly bound to the amino group, which itself acts as a hydrogen bond donor. This reinforces the basic character of the amino group through cooperative effects.

We should notice here that, as it was the case for the head to head complexes, the insertion complexes built from A_I are slightly less bonded than the corresponding structures built from A_{II}.

- Addition structure

The "addition" complex (scheme 2 c-) consists in the opening of the methyl lactate intramolecular hydrogen bond and the formation of an intermolecular hydrogen bond from the hydroxyl group of methyl lactate to the oxygen atom of AI. The intramolecular hydrogen bond of AI remains intact. For this reason, its deformation energy is weaker than that of the previously described structures. The calculated spectra show frequencies in the 3350-3450 cm^{-1} range, typical of intermolecular OH_{ML}…OH_{AI} and intramolecular OH_{AI}…N interactions. It is to be noticed that the AI ν(OH) frequency is lower in the complex than in isolated AI.

Indeed, the formation of the intermolecular hydrogen bond reinforces the intramolecular AI hydrogen bond due to cooperative effects [11].

The addition/AI_{II}-G complex shown in fig. S1e- is an "addition" structure built from AI_{II} and G methyl lactate. The cooperative effects mentioned above are especially important in this complex: the distance between the H of the AI hydroxyl group and the N atom of AI decreases from 2.16 Å in the isolated molecule to 2.04 Å in the complex. The binding and deformation energies amount to 11.14 and 1.21 kcal/mol, respectively. The calculated vibrational spectrum given in fig. S2e- strongly differs from that observed for the previously described complexes. The two main features are located at 3364 and 3449 cm^{-1}. The two stretching modes associated with these values result from an in- and out-of-phase combination of the OH stretching modes of AI and methyl lactate. However, the 3364 cm^{-1} frequency is more localized on the AI moiety and that at 3449 cm^{-1} on methyl lactate. The same geometry has been observed for the system α-methyl-2-naphthalenemethanol/methyl lactate[12].

We can notice here that no "addition" complex containing AI_I or Syn methyl-lactate has been obtained with a binding energy larger than 10 kcal/mol.

- Cycle structure

The "cycle" structure (scheme 2 d-) is characterised by the formation of two intermolecular hydrogen bonds. A hydrogen bond is formed from NH to the O atom of the hydroxyl group of methyl lactate, which in turns acts as a donor towards the O atom of AI. The intramolecular hydrogen bond of AI remains intact and is even reinforced, while the methyl lactate intramolecular hydrogen bond is either slightly or totally opened. This structure is akin to that observed for the AI hydrates[10].

The cycle bifurcated/AI_{II}-G' complex (fig. S1i-) has a binding and deformation energy of 10.63 and 1.63 kcal/mol, respectively. Its vibrational spectrum is depicted in fig. S2i. As it was the case for the addition/AI_{II}-G complex, this spectrum is very different from the one of

insertion or head to head complexes. The feature at 3554 cm^{-1} corresponds to the $\nu(OH_{AI})$ stretch. The two bands at 3442 and 3449 cm^{-1} result from an in- and out- of phase combination of the methyl lactate ν(OH) stretch and the NH_{as} stretch mode of AI. It is to be noticed that these frequencies are higher in energy than those calculated for the addition complex, which is related to larger constraints.

Fig. S1l- shows the "cycle" complex between AI_{II} and the G conformer of methyl lactate. Its binding energy is 10.12 kcal/mol and its deformation energy is equal to 0.77 kcal/mol. Its calculated vibrational spectrum, depicted in fig. S2l-, shows two main vibrations located at 3476 and 3511 cm^{-1}. They correspond to the coupled OH stretch modes of AI_{II} and G.

No "cycle" complex containing AI_I or Syn methyl-lactate has been obtained with a binding energy larger than 10 kcal/mol.

- Other structures

The less stable structure taken into account here is the so called "parallel" complex between AI_{II} and the Syn conformer of methyl lactate. For this complex (fig. S1m-), the intramolecular bond of AI does not open up completely but becomes a bifurcated hydrogen bond between the NH group of AI and the O atom of the methyl lactate hydroxyl. In addition, an intermolecular hydrogen bond is formed between NH and the $O_{C=O}$ of methyl lactate. Fig. S2m- shows the calculated vibrational spectrum associated with this structure, the main frequencies are located at 3358, 3448, 3544 and 3580 cm^{-1}. The first two frequencies correspond to the NH_s and NH_{as} stretch modes, which gain intensity through hydrogen bond formation. The 3544 and 3580 cm^{-1} vibrations are localised on the hydroxyl groups of AI and methyl lactate, respectively, and are slightly coupled.

No "parallel" complex containing AI_I or G methyl-lactate has been obtained with a binding energy larger than 10 kcal/mol.

I.2.b. RR complexes

Most of the structures obtained for the RS diastereoisomer find their counterpart in those calculated for the RR diastereoisomer, eventually with differences in their binding energies. These complexes will not be described again here but their binding, deformation energies as well as their calculated frequencies are given in table S1. However, one structure with binding energy larger than 10 kcal/mol has been found for RR and not for RS. In what follows, we will concentrate on this new complex. We will describe its structure and outline the main other differences between the results obtained for the RS and RR diastereoisomers.

The "new" complex consists of a "cycle" structure formed between AI_{II} and the Syn conformer of methyl lactate (fig. S3a-). Its binding and deformation energies are 10.66 and 0.58 kcal/mol, respectively. In this case, two intermolecular hydrogen bonds ($NH\ldots OH_{ML}$ and $OH_{ML}\ldots OH_{AI}$) are formed between the two moieties. The formation of the $NH\ldots OH_{ML}$ intermolecular hydrogen bond leads to an increase of the oscillator strength associated with the NH_s and NH_{as} stretches. The NH_s vibrational mode is located at 3329 cm^{-1} while the NH_{as} stretch is coupled with the two OH stretches, which gives rise to the 3449, 3457 and 3499 cm^{-1} vibrational modes. We can mention that this complex displays a $CH\ldots\pi$ interaction which adds to its stability. This favourable $CH\ldots\pi$ interaction could not be achieved in the other diastereoisomer for stereochemical reasons and the binding energy of the RS-cycle/AI_{II}-Syn complex (fig. S3b-) falls down to 9.46 kcal/mol.

The more important difference between the RR and RS diastereoisomers concerns the addition/AI_{II}-G of the RS diastereoisomer, which does not belong to the complexes with binding energy larger than 10 kcal/mol for the RR diastereoisomer. Indeed, the binding energy of the addition/AI_{II}-G structure is considerably decreased by interchanging the methyl group and the hydrogen atom located on the asymmetric carbon. The RR addition/AI_{II}-G' complex obtained doing this has been added to table S1 for the sake of comparison. Its binding and deformation energies amount to 9.10 and 0.56 kcal/mol, respectively. The

geometries of the addition/AI_{II}-G complexes for the two diastereoisomers are shown in fig. S3c- and S3d-. It allows us to evidence that the CH…π hydrogen bond disappears when going from RS to RR. This is related to a decrease of the binding energy by 2.04 kcal/mol.

Finally, the cycle/AI_{II}-G complex is strongly more stable for RR than for RS diastereoisomer. Indeed, by performing the methyl/H exchange in the (RS) cycle/AI_{II}-G structure (fig. S3e-), we should have obtained the (RR) cycle/AI_{II}-G' complex. However, it appears than during re-optimisation of the complex structure, G' methyl lactate undergoes isomerisation toward the G conformer, so that both RS-cycle/AI_{II}-G and RS- cycle/AI_{II}-G' correspond to the RR-cycle/AI_{II}-G. The binding energy of this latter structure is higher by 1.49 kcal/mol than that of the RS-cycle/AI_{II}-G. Comparison between fig. S3e- and S3f- shows that an additional CH…π can be formed in the RR complex and not in the RS one, and is responsible for this increase.

I.2.c. Isomerization between different structures

The calculated RS insertion/AI_{II}-G and the closely related RS insertion/AI_{II}-G*bis* complexes display very similar characteristics both in term of energetic and calculated frequencies. Moreover, we have calculated that RS insertion/AI_{II}-G*bis* can undergo isomerization toward the more stable RS insertion/AI_{II}-G complex with a very low barrier of 0.36 kcal/mol. So these two complexes will not co-exist in the expansion. Similarly, the RR insertion/AI_{II}-G' or RR insertion/AI_{II}-G'*bis* complexes will not co-exist as the interconversion between them is a process involving a low barrier. It is to be noted that the G and G' conformers of ML are physically very similar. Indeed, the rotational barrier between G and G' has been evaluated around 0.5 kcal/mol [13].

References :

[1] K. Le Barbu-Debus, M. Broquier, A. Mahjoub, and A. Zehnacker-Rentien, Journal of Physical Chemistry A **112** (40), 9731 (2008).

[2] K. Le Barbu-Debus, N. Seurre, F. Lahmani, and A. Zehnacker-Rentien, Physical Chemistry Chemical Physics **4**, 4866 (2002).

[3] P. Claverie, *Intermolecular Interactions from diatomics to biopolymers*. (Pullman B., Ed.; Wiley, New York, 1978).

[4] V. Brenner and P. Millié, Zeitschrift für Physik D **30**, 327 (1994).

[5] K. Le Barbu, V. Brenner, P. Millié, F. Lahmani, and A. Zehnacker-Rentien, Journal of Physical Chemistry A **102**, 128 (1998).

[6] N. Metropolis, A. Rosenbluth, A. Teller, and E. Teller, Journal of Chemical Physics **21**, 1087 (1953).

[7] M. J. Frisch, G. W. Trucks, H. B. Schlegel, G. E. Scuseria, M. A. Robb, J. R. Cheeseman, J. A. Montgomery, T. V. Jr., K. N. Kudin, J. C. Burant, J. M. Millam, S. S. Iyengar, J. Tomasi, V. Barone, B. Mennucci, M. Cossi, G. Scalmani, N. Rega, G. A. Petersson, H. Nakatsuji, M. Hada, M. Ehara, K. Toyota, R. Fukuda, J. Hasegawa, M. Ishida, T. Nakajima, Y. Honda, O. Kitao, H. Nakai, M. Klene, X. Li, J. E. Knox, H. P. Hratchian, J. B. Cross, C. Adamo, J. Jaramillo, R. Gomperts, R. E. Stratmann, O. Yazyev, A. J. Austin, R. Cammi, C. Pomelli, J. W. Ochterski, P. Y. Ayala, K. Morokuma, G. A. Voth, P. Salvador, J. J. Dannenberg, V. G. Zakrzewski, S. Dapprich, A. D. Daniels, M. C. Strain, O. Farkas, D. K. Malick, A. D. Rabuck, K. Raghavachari, J. B. Foresman, J. V. Ortiz, Q. Cui, A. G. Baboul, S. Clifford, J. Cioslowski, B. B. Stefanov, A. L. G. Liu, P. Piskorz, I. Komaromi, R. L. Martin, D. J. Fox, T. Keith, M. A. Al-Laham, C. Y. Peng, A. Nanayakkara, M. Challacombe, P. M. W. Gill, B. Johnson, W. Chen, M. W. Wong, C. Gonzalez, and J. A. Pople, Gaussian 03, Revision C.02, (Gaussian, Inc., Wallingford CT, 2004., 2003).

[8] S. Boys and F. Bernardi, Molecular Physics **19**, 553 (1970).

[9] K. S. Kim, P. Tarakeshwar, and J. Y. Lee, Chemical Reviews **100**, 4145 (2000).

[10] K. Le Barbu-Debus, N. Guchhait, and A. Zehnacker-Rentien, Physical Chemistry Chemical Physics **9** (32), 4465 (2007).

[11] F. C. Hagemeister, C. J. Gruenloh, and T. S. Zwier, Journal of Physical Chemistry A **102** (1), 82 (1998).

[12] N. Seurre, K. Le Barbu-Debus, F. Lahmani, A. Zehnacker, N. Borho, and M. A. Suhm, Physical Chemistry Chemical Physics **8**, 1007 (2006).

[13] A. Borba, A. Gomez-Zavaglia, L. Lapinski, and R. Fausto, Vibrational Spectroscopy **36** (1), 79 (2004).

Table S1: Binding and deformation energies obtained for the complexes calculated at the MP2/6-31(d,p) level of theory together with the harmonic frequencies of significant intensities calculated at the B3LYP/6-31G(d,p) level. The energies are given relative to the closest most stable fragments (see text).

RS	D_e	**BE**	E_{def} AI	E_{def} ML	ν(OH)	ν(OH)	ν(NH)
head to head bifurcated/AI_{II}-G'	-16.34	**-12.59**	1.39	1.99	3153	3537	
head to head/AI_{II}-Syn	-15.34	**-11.93**	1.68	2.83	3139	3521	
insertion/AI_{II}-Syn [a)]	-15.11	**-11.39**	1.34	2.42	3068	3506	
insertion/AI_{II}-G	-14.87	**-11.38**	1.81	1.30	3181	3522	
addition/AI_{II}-G	-15.34	**-11.14**	0.34	1.21	3364	3449	
insertion/AI_{I}-G	-15.11	**-11.13**	2.48	2.12	3110	3525	
insertion/AI_{II}-G*bis*	-14.04	**-10.87**	1.57	1.05	3166	3488	
head to head/AI_{I}-Syn	-14.35	**-10.80**	3.19	2.70	3139	3534	
cycle bifurcated/AI_{II}-G'	-14.80	**-10.63**	0.49	1.63	3442	3449	3554
insertion /AI_{I}-Syn	-14.27	**-10.42**	2.43	2.60	3044	3509	
head to head/AI_{II}-G	-12.96	**-10.23**	1.31	1.81	3229	3563	
cycle/AI_{II}-G [b)]	-14.41	**-10.12**	0.28	0.77	3476	3511	
parallel/AI_{II}-Syn	-14.20	**-10.07**	0.46	0.47	3544	3580	
cycle /AI_{II}-G'	-13.18	**-9.83**	0.24	0.37	3491	3510	
cycle/AI_{II}-Syn	-13.83	**-9.46**	0.43	0.63	3453	3459	3487
RR	D_e	**BE**	E_{def} AI	E_{def} ML			
head to head bifurcated/AI_{II}-G	-16.40	**-12.74**	1.39	2.11	3159	3560	
head to head/AI_{II}-Syn	-15.57	**-12.14**	1.62	2.94	3075	3512	
cycle/AI_{II}-G	-16.07	**-11.61**	0.48	0.32	3482	3505	
insertion/AI_{II}-G'	-15.04	**-11.48**	1.81	1.15	3178	3522	
insertion/AI_{I}-G’	-15.10	**-11.04**	2.43	1.96	3119	3523	
insertion/AI_{II}-G’*bis*	-14.18	**-10.93**	1.62	0.82	3173	3501	
cycle/AI_{II}-Syn	-15.25	**-10.66**	0.58	0.58	3449	3457	3499
head to head/AI_{I}-Syn	-14.27	**-10.66**	3.08	2.49	3146	3536	
insertion/AI_{I}-Syn	-14.38	**-10.49**	2.42	2.41	3031	3505	
cycle bifurcated/AI_{II}-G	-14.18	**-10.26**	0.40	1.66	3442	3451	3549
head to head/AI_{II}-G'	-12.75	**-9.79**	0.74	1.09	3311	3579	
parallel/AI_{II}-Syn	-14.00	**-9.53**	0.60	1.26	3081	3513	
addition/AI_{II}-G’	-12.68	**-9.10**	0.30	0.56	3385	3474	

a) re-optimisation of RR-insertion/AI_{II}-Syn gives RR-head to head/AI_{II}-Syn complex

b) re-optimisation of RR-cycle/AI_{II}-G’ gives RR-cycle/AI_{II}-G

Figure caption

Figure S1: Calculated complexes for the (1R,2S)-(+)-cis-1-amino-2-indanol/S-methyl lactate diastereoisomer. a-) Head to head bifurcated/AI_{II}-G', b-) Head to head/AI_{II}-Syn, c-) Insertion/AI_{II}-Syn, d-) Insertion/AI_{II}-G, e-) Addition/AI_{II}-G, f-) Insertion bifurcated/AI_{I}-G, g-) Insertion/AI_{II}-G, h-) Head to head/AI_{I}-Syn, i-) Cycle bifurcated/AI_{II}-G', j-) Insertion/AI_{I}-Syn, k-) Head to head/AI_{II}-G, l-) Cycle/AI_{II}-G and m-) Parallel/AI_{II}-Syn

Figure S2: Calculated spectra for the (1R,2S)-(+)-cis-1-amino-2-indanol/S-methyl lactate diastereoisomer (scaled B3LYP/6-31G(d,p) harmonic frequencies convoluted by a Lorentzian line shape of 6 cm^{-1} FWMH) a-) Head to head bifurcated/AI_{II}-G', b-) Head to head/AI_{II}-Syn, c-) Insertion/AI_{II}-Syn, d-) Insertion/AI_{II}-G, e-) Addition/AI_{II}-G, f-) Insertion bifurcated/AI_{I}-G, g-) Insertion/AI_{II}-G, h-) Head to head/AI_{I}-Syn, i-) Cycle bifurcated/AI_{II}-G', j-) Insertion/AI_{I}-Syn, k-) Head to head/AI_{II}-G, l-) Cycle/AI_{II}-G and m-) Parallel/AI_{II}-Syn. Experimental spectra are given for the sake of comparison.

Figure S3: Selected calculated structures for the (1R,2S)-(+)-cis-1-amino-2-indanol/R-methyl lactate diastereoisomer, for comparison with the structures of the equivalent (1R,2S)-(+)-cis-1-amino-2-indanol/S-methyl lactate diastereoisomer. a-) RR Cycle/AI_{II}-Syn, b-) RS Cycle/AI_{II}-Syn, c-) RR Addition/AI_{II}-G', d-) RS Addition/AI_{II}-G, e-) RR Cycle/AI_{II}-G and f-) RS Cycle/AI_{II}-G'.

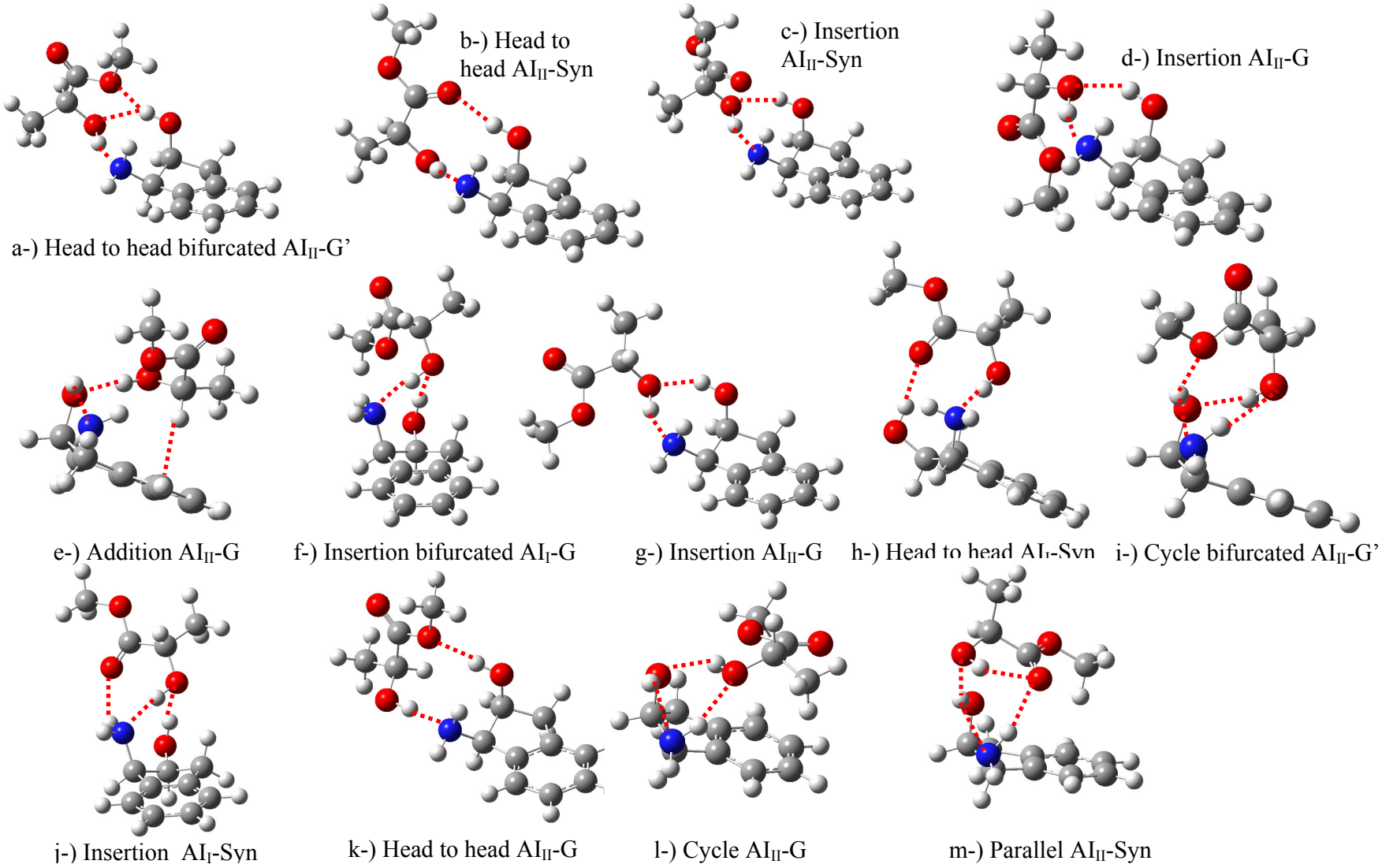

Figure S1 :

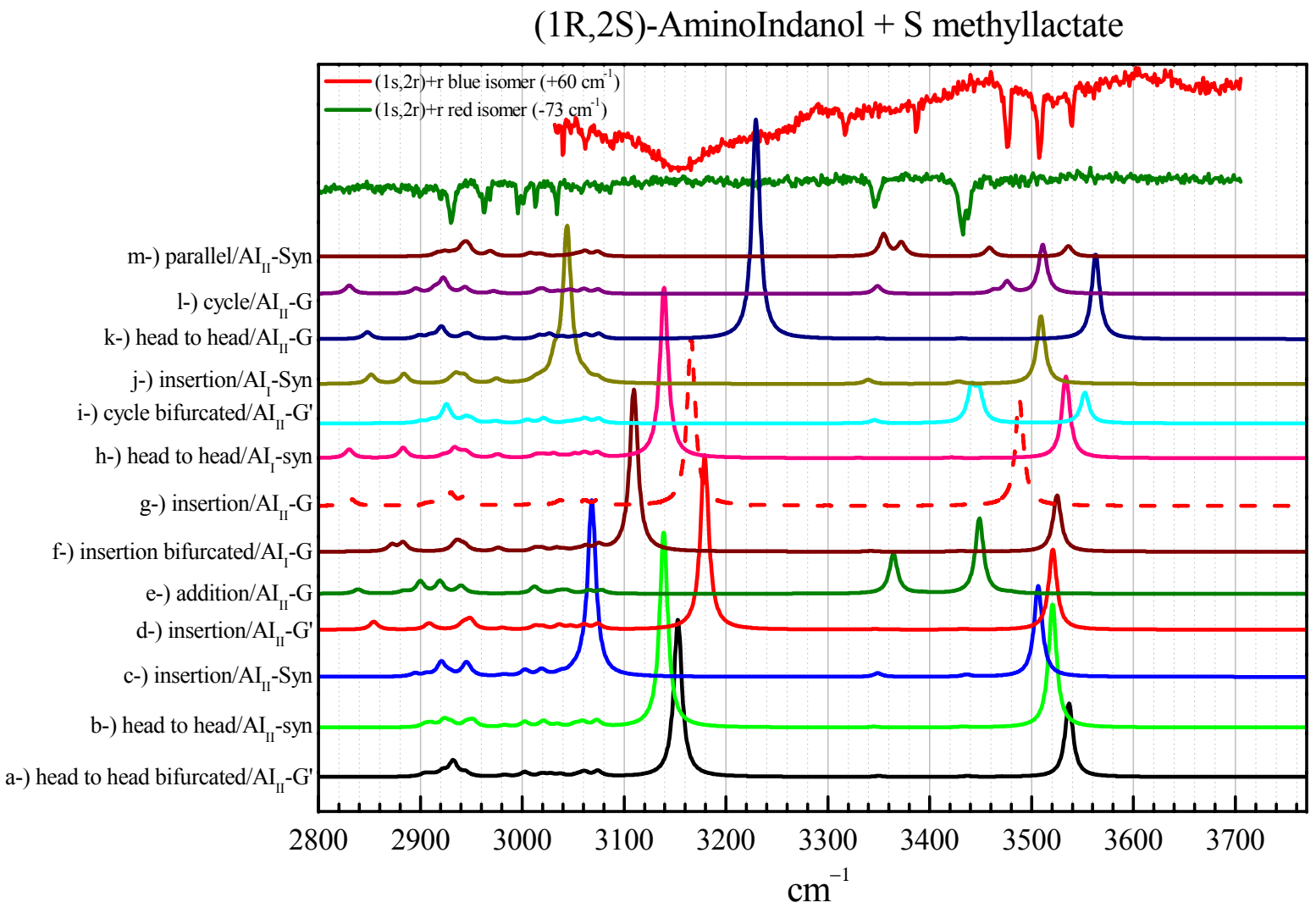

Figure S2 :

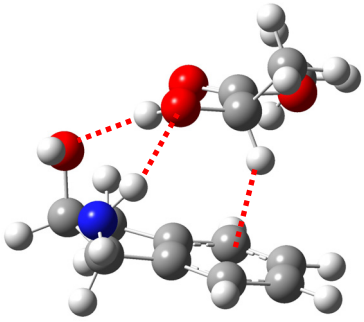

a-) RR Cycle AI_{II}-Syn

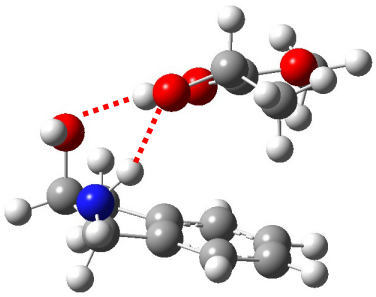

b-) RR Cycle AI_{II}-Syn

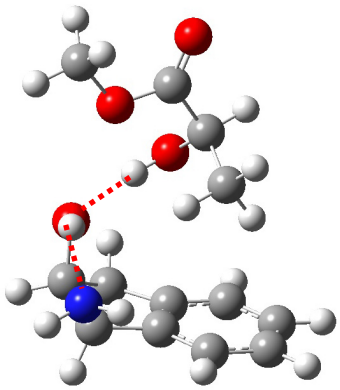

c-) RR Addition AI_{II}-G'

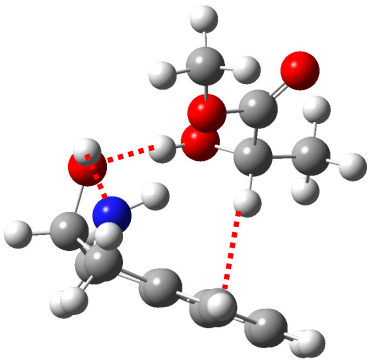

d-) RS Addition AI_{II}-G

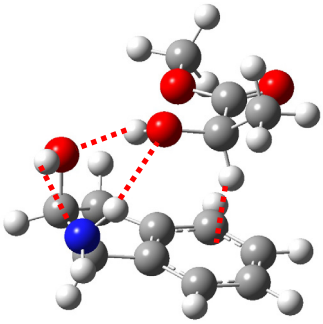

e-) RR Cycle AI_{II}-G

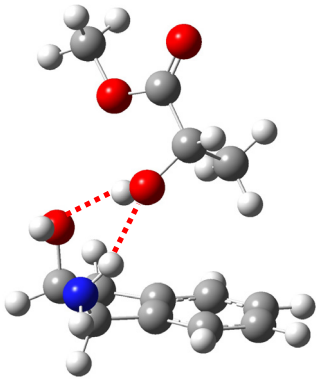

f-) RS Cycle AI_{II}-G'

Figure S3